Phase II: Developing of the experimental model for the laser pyrolysis synthesized TiO_2-based nanoparticles which containmaghemite/magnetite-type iron oxide as the magnetic core (using the $Fe(CO)_6$ precursor) embedded in a TiO_2 matrix; synthesis and characterization

TiO_2 is extensively studied for its wide (among others) applications in photochemistry and photocatalysis (for example), as an excellent UV absorber in [1] for indoor applications [2] for antimicrobial activity [3] or wastewater treatment [4,5]. In photocatalytic appplications, the TiO_2 activity is limited due to the high rate of recombination of pairs e^- /h $^+$ (negative electrons and positive holes) [6]. In pure TiO_2, the average lifetime of electron-hole pairs is about 30 ns. The titania doping with 0.5% Fe (III) markedly increases the lifetime of charge carriers, extending to minutes and even hours [8-10].

Our synthesis technique is based on the resonance between the laser emission line of a CW CO_2 laser and the absorption band of a gas precursor. In this paper we report the synthesis of TiO_2 nanocompounds doped with Fe species using the laser pyrolysis synthesis method. There were two separate series of experiments conducted in order to verify the evidence of magnetism in two different experimental situations:

1. In the first case, the SCF sample, the flow of iron carbonyl enters the reaction zone in a mixture with the precursor of titanium ($TiCl_4$) by the median nozzle.

2. In the second case, the IT sample, pentacarbonyl iron vapors flow enters in the reaction zone through the central nozzle, being thus separated from the other reactants along the installation, and having the meeting with the rest of the reactive mixture only after leaving the nozzle , directly in the reaction zone (the laser pyrolysis "flame").

The main experimental parameters are listed in Tables I and II. In the last column of the table are marked EDX elemental measurement results (in at%). Nanostructured titanium oxide doped with Fe-based phases were characterized by various analytical methods (XRD, TEM, EDX, magnetic measurements).

Table I and II – Experimental parameters (I – SCF sample; II – IT sample)

Nr exp	ΦArf [sccm]	ΦArconf [sccm]	Φaer [sccm]	Φ_{C2H4} [sccm]	$\Phi_{Ar\rightarrow Fe(CO)5}$ [sccm]	P [mbar]	P [W]	T [min]	M [g]	P [g/h]	EDAX (Fe/Ti %) (average)
SCF 2-1	650	1100	150	100	10	450	400	210	1.70	0.485	23 (±3)
SCF 5-1	550	1100	150	100	6	450	400	180	2.10	0.700	12 (±3)
SCF-B1	1300	1500	225	150	5(3)	450	400	60	0.83	0.83	4 (±2)

Nr. Ex.	Φ_{Arf} [sccm]	Φ_{Arconf} [sccm]	$\Phi_{aer\rightarrow TiCl4}$ [sccm]	$\Phi_{C2H4\rightarrow TiCl4}$ [sccm]	$\Phi_{C2H4\rightarrow Fe(CO)5}$ [sccm]	P [W]	P [mbar]	M [g]	T [min]	OBS.
IT-1	1700	2000	300	45	30	600	450	3.31	140	
IT-2	1700	2000	300	45	30	450	350	0	30	
IT-3	1700	2000	300	45	30	450	450	1.41	35	

IT-4	1700	800	350	50	50	400	450	17.09	240	We changed the central nozzle

From the UV-Vis absorption curves is observed that the absorbance is larger and has a red-shift with increasing dopant concentration. Maximum bandwidth narrowing (bandgap) is estimated at 2.32 eV and the maximum concentration occurs in the Fe dopant. The XRD analysis of titanium samples reveals the coexistence of anatase and rutile phases.

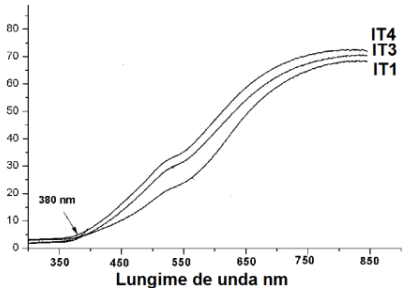

Fig. 1. UV-Vis spectral response in samples of type IT: curves correspond to different doping ratios of Fe / Ti (Table II)

Observing the X-ray diffractograms of IT samples (Fig. 2b) reveals that most Fe compounds would find less IT-1 and IT-3. This seems at odds with the results of EDX. However, an explanation of the differences between IT1 and IT3 may find that they can form different compounds based on iron $Fe_xTi_yO_z$ (and not only metallic iron). In terms of TiO_2, the anatase and road quantities are not different in IT1 towards IT3 sample.

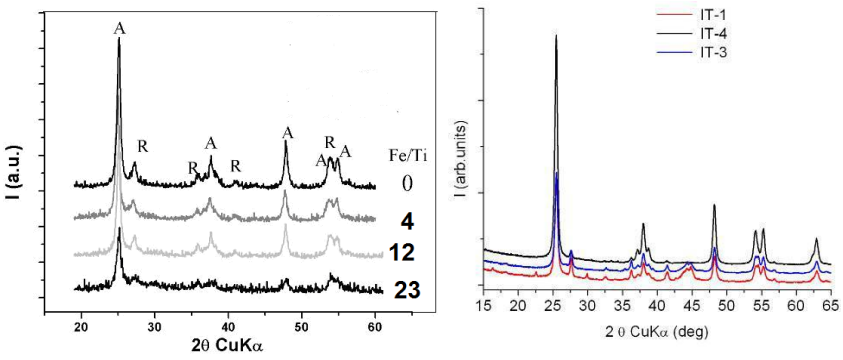

Fig. 2a and b. XRD patterns of SCF-a and IT-b samples

In fig. 2a one can see the evolution of diffraction curves for the system Fe-doped TiO_2 particles with atomic ratio Fe / Ti between 0 and 23%. An important feature of this image is high intensity peak of anatase (101), an indicator of a higher crystallinity compared to other doped samples. A major effect of doping appears to be decreasing crystalline anatase-TiO_2

phase with the increasing Fe concentration and, consequently, an increase in the amorphous phase (and also of the rutile phase).

From the X-Ray diffractogrames analyses result the characteristic crystallographic properties of these powders, collected in table 2. The presence of convoluted peaks around 2θ = 38 degrees probably implies the overlapping of different traces several phases and highlights different levels. Thus, in samples IT-1 and IT-3 appears probable iron carbide Fe_3C phase (especially in IT-1 sample).

Another crystalline phase, which occurs throughout the IT-1 and IT3 samples is magnetite- Fe3O4 phase type (or magnetic titanium Fe ($Fe_{1.17}Ti_{0.54}$) O_4 titanomagnetite or titanomaghemite distinguished by constant network due to its substitution of $Fe^{3+}$with Ti^{4+}).

Semi-quantitative elemental analysis EDAX (Fig. 3) was used to determine the atomic ratio in TiO_2-based nanopowders (see last column of Table 1 and Table II and IV). Considering the uncertainty, the values of Fe / Ti doped samples can be found in a qualitative estimation.

Sample	**TiO_2**				**P(W)**	**Fe/Ti**
	A (%)	**R (%)**	**D_A (nm)**	**D_R (nm)**		
IT-4	96	4	23	28	400	0.018
IT-1	81	19	22	33	600	0.358
IT-3	81	19	25	33	450	0.481

Table III. Crystallographic properties deduced from studies of samples by X-ray diffraction (XRD)

Sample	**Fe**	**Ti**	**O**	**C**
IT-1	6.52	18.23	35,53	39.72
IT-3	9.62	20.00	42.73	27.65
IT-4	0.41	22.26	35.58	41.75

Table IV. The elemental composition of the IT samples, estimated by EDX analysis (in at%)

High resolution TEM images of IT synthesized samples show bigger or smaller groups of nanoparticles especially rounded (although polyhedral shapes appear) (see Figures 4 and 5). The Fe doped TiO_2 nanoparticle images show no semnificative differences in powder morphology between IT1 and IT3 (possibly simplify the coating layers in the latter case). Interplanar distances marked on Figure 5 correspond to anatase TiO_2 and metallc Fe planes. It is assumed that certain crystallographic shear planes that appear in the image on the right (fine sheets appear to have different structures and compositions) would belong surface defects due to traces of non-stoichiometric TiO_2.

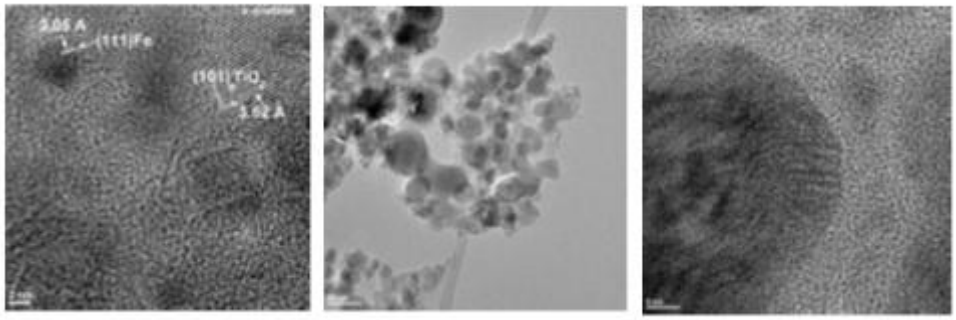

Fig. 4 a,b and c. High resolution images for IT-1sample: planar distances are shown corresponding planes (101 of anatase and the corresponding planes (111) consisting of Fe particles most likely one (or more) hard cores and of several coatings (most likely a turbostratic carbon layer on the outside)

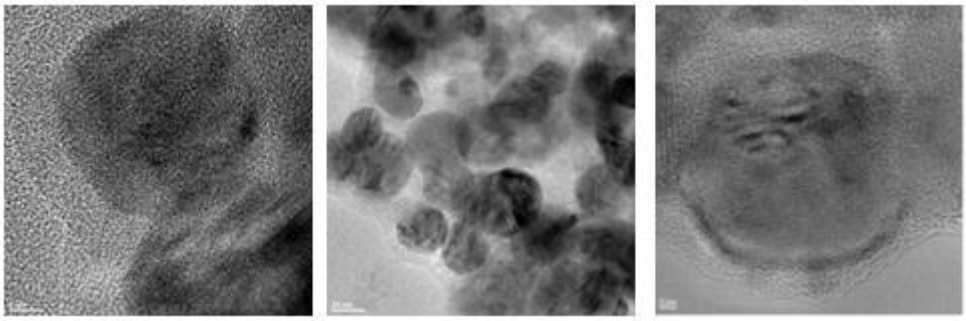

Fig. 5 a,b and c. High resolution images for IT-3 sample: identify core-shell particles, seeming to present a common part, coalesced; and most likely composed from more hard cores (dark contrast)

In terms of magnetic properties, the emphasis in this report on the evidence of type II, generically called IT, because they exhibit magnetic properties, thus registering a first success of the underway project (one of the main objectives is the architecture new nano-TiO_2 magnetic properties.

All samples show a similar magnetic behavior at low-field cooling (FC 100 Oe), consisting of a slight quasi-linear increase of the magnetization by lowering the temperature down to 50 K, specified to a magnetic ordered state and a hyperbolic growth (1/T type) up to 5 K, specific to a paramagnetic state. These informations can be interpreted as a superposition of two differentt magnetic phases, a ordered one up to room temperature and another one with tendency to a paramagnetic relaxation, which is ended around 50 K. The Mossbauer spectra show the presence at the lowest temperature of a magnetic state (accompanied by a paramagnetic one). The initial magnetic state undergoes a rapid relaxation up to 50 K, where

all the iron-base phases become paramagnetic. The phase which shows a magnetic ordering at room temperature is not correlated with the iron-rich phases, allowing thus to conclude that we have a magnetic diluted oxide (DMO) which can appear due to de defects in the TiO_2 matrix.

The SCF-2 sample shows an only 20 Oe coercitive field at low temperatures, value slighthy that slightly diminishes at higher temperatures, which is an indication of the insignificant presence of an ordered magnetic phase. Yet, the SCF-5 sample, with a much lower iron percentage has a coercive field of 60 Oe (at low temperatures and which also slightly diminishes with the temperature increasing). Thus, the magnetic oriented phase of SCF-5 have a higher contribution than those from SCF-2, in spite of their lower iron content. On the other hand, the SCF-5 powder has a higher anatase content, so this phase is the origin of those special type of magnetism, characteristic to a DMO system. The diamagnetic contribution at room temperature of the SCF-5 sample is strong as espected, since the iron content is also lower, which induce a paramagnetic contribution lower than the diamagnetic one (at higher temperatures). The SCF-1 powder show a 170 Oe coercive field at low temperature (with a weak decreasing tendency towards higher temperatures) and also here it is a dignature of DMO behavior. At high field cooling of this sample, the coercive field increases to 240 Oe, with a negative shift of 80 Oem suggesting the involving of an exchange bias effect as the result of interaction between DMOO phase and an antiferromagnetic one al low temperatures. Regarding the Mossbauer spectra which respond only to the presence of Fe atoms or ions, all SCF samples shows the existence of two magnetic phase and a paramagnetic one at the lowest temperature (5K). As extracted from the hyperfine parametres, the magnetic phase with a 44 T field and izomer shift of 0.53 mm/s at 5K can be attributed to oxohydroxyde phase β-FeOOH - nonstoechiometric akaganeite, whereas the other magnetic phase with a 24 T field phase with a izomeric shift of 0.1-0.2 mm/s can be attributed to a iron carbide (similar to Fe_3C cementite). Both these two phases become superparamagnetic above 50K due to the very small nanoparticle size (few nm). The third phase, a paramagnetic one (at 5K) can be attributed to Fe dissolved in the TiO_2 matrix or can be seen as an superparamagnetic alternative of one of the FeOOH or Fe-C phase. From the values of the isomeric shift of 0.49 mm/s and quadrupolar shift of 0.70 mm/s the most probable attribution for this phase is β-FeOOH. The Fe_3C phase (supeparamagnetic above 50K) accounts for 14% from all Fe-containing phases, whereas the magnetic phase β-FeOOH (at 5 K) accounts for 40% for SCF-B1 (whereas is only 12% in SCF-5 and 35% for SCF-2). The bulk akaganeite phase found in nature is antiferromagnetic and their higher proportion in SCF1 powder can be the reason for the presence of the exchange-bias only in this sample. The presence of paramagnetic/superparamagnetic and antiferromagnetic phases at room temperature signifies that the SCF sample have a weak or absent response to external magnetic fields.

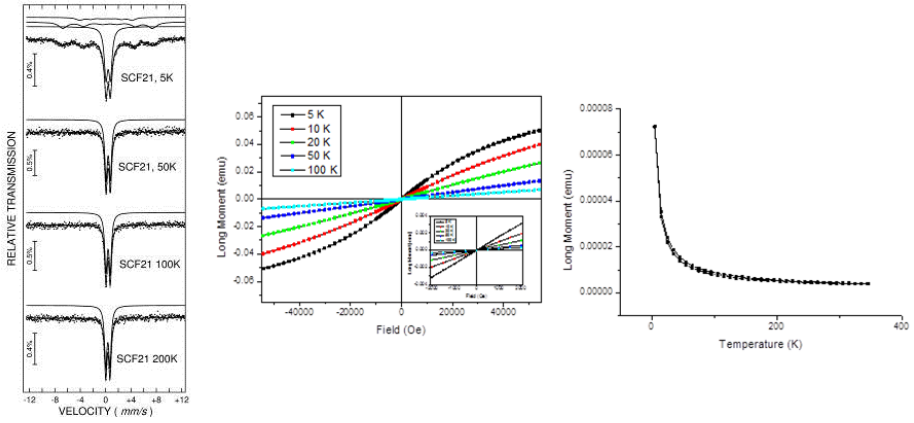

Fig. 6. Magnetic measurements for SCF2 sample

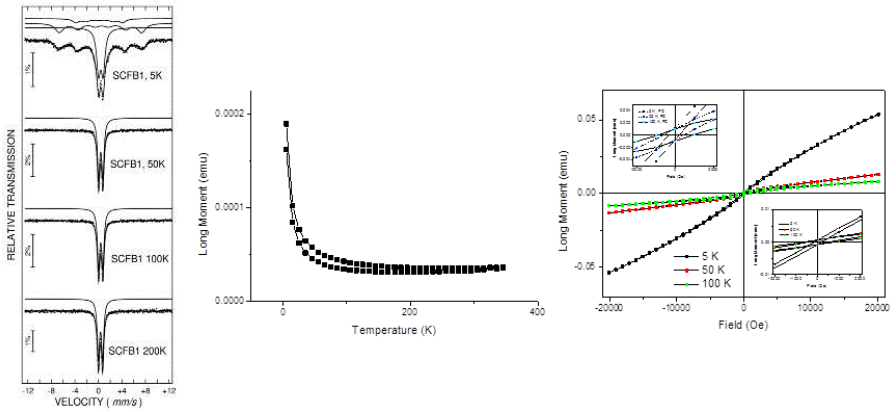

Fig. 7. Magnetic measurements for SCF-B sample

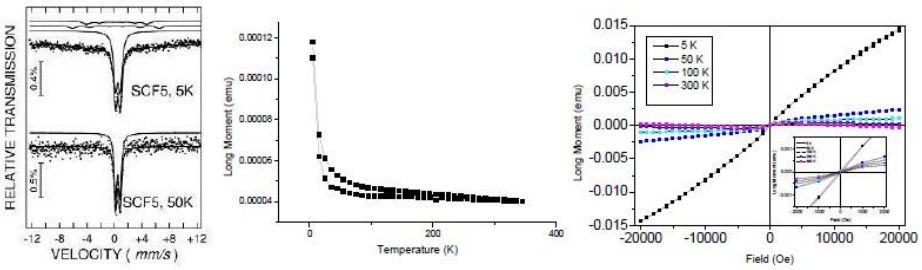

Fig. 8. Magnetic measurements for SCF5 sample

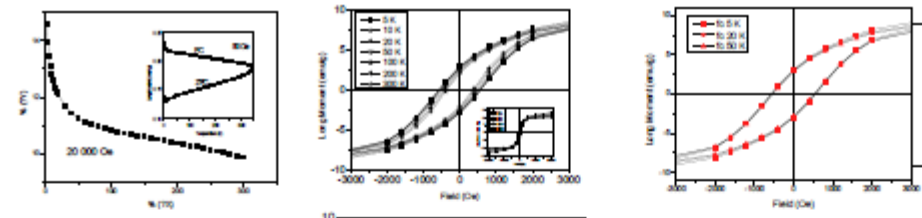

Fig. 9 a, b si c. Masuratori magnetice pentru proba IT 1

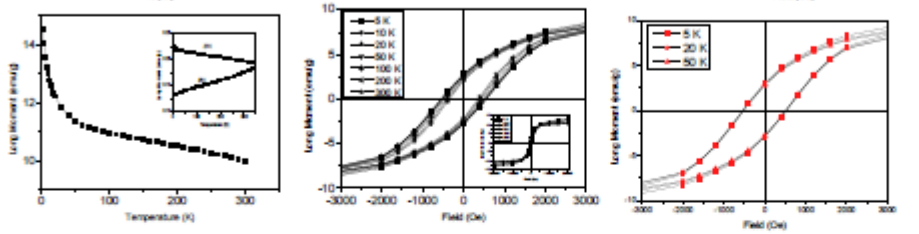

Fig. 10 a, b si c. Masuratori magnetice pentru proba IT 3

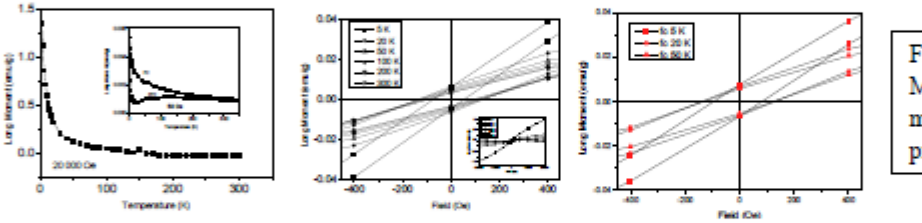

Fig. 11a, b si c. Masuratori magnetice pentru proba IT 1

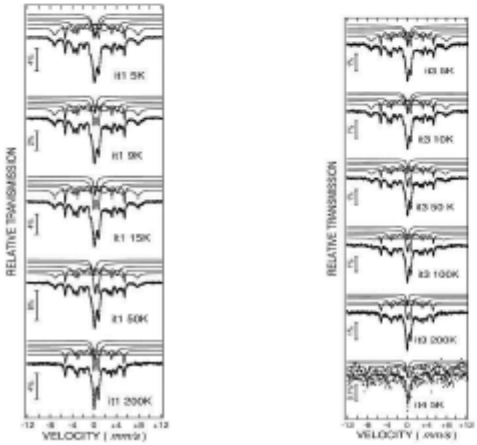

Fig. 12 a, b . Spectrul Mossbauer la diferite temperaturi: a- pentru proba IT1; b- pentru proba IT3, care prezinta in partea inferioara spectrul la 5K pentru proba IT4

The method of developing of magnetic particles of TiO_2 photocatalytic activity in specific aqueous phase

The samples were heat treated at 450°C. Preliminary tests evaluation of UV photoactivity of the samples were performed by scanning electrochemical microscopy (SECM Microscopy Electrochemical Scanning) which determine the evolution of oxygen consumed in the presence of pollutant para-chlorophenol. We have tested SCF samples,which present the results in Fig.14below.

Photocatalytic testing from IT samplesis being check reproducibility. Since samples containing carbon (unwanted decomposition of ethylene senzitivantului), are presented first results of photocatalytic degradation in UV light (see Figure 15) for the sample with the lowest carbon content of Fe.

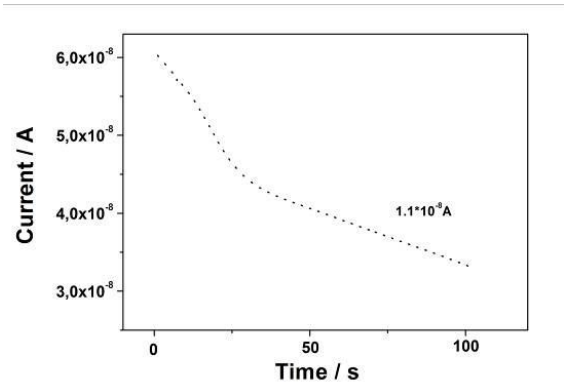

Fig.14. SECM measurements for picking transient response to Pt micro-electrode, placed over a film from SCF-B sample

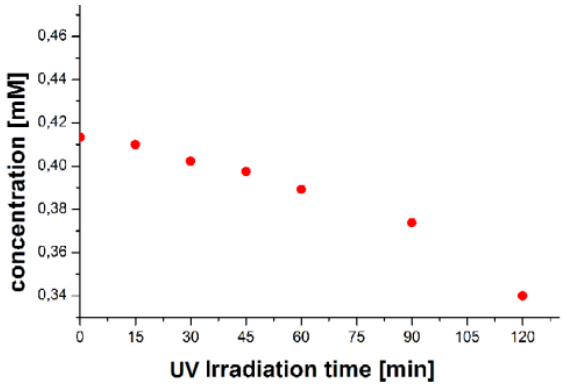

Fig.15. Pollutant degradation of salicylic acid in the presence of C and Fe-doped TiO_2particles

The nanoparticles were mixted with salycilic acid solution and keeped at dark for 30 minutes for the attaining of the adsorption-desorbtion equilibrium.

We used a UV lamp (400W) and followed standard procedure for photocatalysis (adding the necessary catalyst to an aqueous solution of salicylic acid, with concentration required). Percentage degradation of the pollutant was derived by measuring the UV absorbance by UV-VIS spectrophotometer.

The most important achievement of this phases both scientific conceptually and objectives of the project is the experimental model of TiO_2-based nanoparticles on synthesized by laser pyrolysis, containing maghemite / magnetite iron oxide or even metallic / carbidic phases as magnetic core. In other words, we succeeded to induce magnetic properties due to metalic/oxidic iron oxide nanophases in photocatalytic-active titania nanocomposites

Referinte

[1] X A. Jaroenworaluck, et. al., Surface and Interface Analysis 38 (2006) 473-477.
[2] P. Pichat, et.al., Catalysis Today 63 (2000) 363-369.
[3] K.S. Yao, et.al., Surface and Coatings Technology 201 (2007) 6882-6885.

[4] I. Lanhua Hu, et. al, Water Research 41 (2007) 2612-2626.
[5] I Oller, et. al., Water Sci Technol. 55 (2007) 229-235.
[6] X. H. Wang, et. al., Journal American. Chemical Society 127 (2005) 10982-10990.
[7] I. Djerdj and A.M. Tonejc, J. Alloys Compd 413 (2006) 159-174.
[8] J. Moser, et. al., Helv. Chim. Acta 70 (1987) 1596-1604.
[9] A.R. Bally, et. al, J. Phys. D 31 (1998) 1149-1154.
[10] F.C. Gennari and D.M. Pasquevich, J. Mater. Sci. 33 (1998) 1571-1578.
[11] W.R. Cannon, et. al., J. Am. Ceram. Soc. 65 (1982) 324-330.
[12] C. Jaeger, et. al., Appl. Phys. A 85 (2006) 53-62.
[13] E. Borsella, et. al., Nanostructured Materials 6 (1995) 341-344.
[14] A.Tomescuet. al, Journal Material Science 42 (2007) 1838-1846.

Management activity, dissemination, editing

a) Scientific paper 2012:

E. Popo vici, C. Luculescu, *R. Alexandrescu*, C. Fleaca, F. Dumitrache, R. Barjega, M. Scarisoreanu, E. Duta, A. Barbut, I. Morjan , Development of systems for the laser synthesis of nanoparticles starting from liquid precursors, Applied Surface Science (Elsevier) Volume 258, Issue 23, 15 September 2012, Pages 9326–9332,
- M. Scarisoreanu, *R. Alexandrescu*, I. Morjan, R. Birjega, C. Luculescu, E. Popovici, E. Dutu, E. Vasile, V. Danciu, N. Herlin-Boime, Structural evolution and optical properties of C-doped TiO2 nanoparticles prepared by laser pyrolysis, Applied Sueface Science (Elsevier) , 2012, in press
- *R. Alexandrescu*, I. Morjan, F. Dumitrache, M. Scarisoreanu, C. T. Fleaca, I. P. Morjan, A. D. Barbut, R. Birjega,G. Prodan, Development of TiO2 and TiO2/Fe-based polymeric nanocomposites by single-step laser pyrolysis, Applied Sueface Science (Elsevier) , 2012, in press

b) International Conferences communications 2012:

-M. Scarisoreanu, *R. Alexandrescu*, I. Morjan, R. Birjega, C. Luculescu, E. Popovici, E. Dutu, E. Vasile, V. Danciu, N. Herlin-Boime, Structural evolution and optical properties of C -doped TiO2 nanoparticles prepared by laser pyrolysis E-MRS 2012 Spring Meeting, Strasbourg, May 14-18, 2012
-*R. Alexandrescu*, I. Morjan, F. Dumitrache, M. Scarisoreanu, C. T. Fleaca, I. P. Morjan, A. D. Barbut, R. Birjega,G. Prodan, Development of TiO2 and Ti/Fe-based polymeric nanocomposites by single-step laser pyrolysis, E-MRS 2012 Spring Meeting, Strasbourg, May 14-18, 2012

c) Invited paper 2012:

R. Alexandrescu,, A. Rotaru, I. Morjan, C. Fleacă, F. Dumitrache, M.Scarisoreanu, Fe-based / methyl methacrylate polymeric nanocomposite prepared by laser pyrolysis: structural and thermal properties, 1st Annual World Congress of Advanced Materials Conference (WCAM-2012), June 6-8, 2012 Beijing, China

Project Director,